A NUMERICAL PROCEDURE FOR COMPUTATION OF OUTGOING TERRESTRIAL FLUX BASED UPON THE ELSASSER-CULBERTSON MODEL WITH TESTS APPLIED TO MODEL-ATMOSPHERE SOUNDINGS

F. L. MARTIN [1] and J. B. TUPAZ, LT. USN [2]

U.S. Naval Postgraduate School, Monterey, Calif.

ABSTRACT

A numerical procedure for the computation of emergent terrestrial flux has been developed after the model described by Elsasser and Culbertson. By application of this procedure, a set of emergent fluxes has been computed for each of 63 soundings drawn from the model atmospheres developed by Wark et al. The latter authors have also made available for this study the results of their radiative model for outgoing intensities. Both radiative models included contributions from atmospheric water vapor, carbon dioxide, and ozone, as well as transmitted interface (cloud or ground) effects. Both sets of fluxes computed for the 63 model atmospheres were subjected to a stepwise-screening multiple linear regression analysis, using empirically tested parameters grossly representative of the radiosondes. In terms of these parameters as independent variables, the fluxes computed by the radiative model of Wark et al. were specified in accordance with a multiple correlation coefficient of 0.98, while the fluxes computed here gave rise to a multiple correlation of 0.625. The chief reason advanced for the smaller statistical specification by the present model, as contrasted with that of Wark et al. is considered to be due to the differing number of sounding levels used in carrying out the two sets of computation.

1. INTRODUCTION

In this paper, two objectives are undertaken. The first is that of devising a computational technique for the total outgoing terrestrial flux closely modeled after that set forth by Elsasser and Culbertson [2]. This objective was considered particularly opportune, since Elsasser and Culbertson had already set forth in tabular form the radiative transfer functions which were to be integrated in their model. In finalizing the computational aspects, there remained only the necessity of introducing a limited number of iterative operations in adapting any sounding to the functions listed by Elsasser and Culbertson (hereafter denoted by EC). Procedural consistency with the EC model has been considered to be of prime importance in the process of adaptation of the model to computer solutions involving soundings.

The second objective is that of applying the adapted EC model to the computation of outgoing terrestrial flux F across the level $p=0.1$ mb. for each of 63 model atmospheres. These model atmospheres were a subset of 106 such atmospheres contained in Appendix A of Wark, Yamamoto, and Lienesch [13]. References to works of these authors will frequently be indicated by the abbreviation WYL. From the WYL intensity computations $I(\theta)$ at the top of the same set of 63 atmospheres, a comparison flux F_{WLY} has been derived for each model atmosphere using

$$F_{WYL}=\pi \int_0^1 I(\theta)\, d\,(\sin^2\theta). \qquad (1)$$

[1] Support by the Navy Weather Research Facility, and Naval Air Systems Command Project Famos is gratefully acknowledged.

[2] Present affiliation: Naval Science Department, Naval Academy, Annapolis, Md.

Some statistical inferences concerning the relative accuracy of flux computations by the two models are drawn in sections 5 and 6.

In deriving their emergent intensities $I(\theta)$, WYL [13, 14] outline first a method for determining band intensity contributions over small wave number intervals (of either 25 cm.$^{-1}$, or of intervals nearly equal to this range), and for $\theta=0°$, 20°, 45°, 78.5°. Equation (7) of [14] affords the framework for this phase of their computations. In performing these computations, WYL have first increased the vertical resolution between the interface of each one of the 106 listed model atmospheres ([13], pp. 51–69) by interpolation of 200 levels between the interface and the top of the atmosphere, $p_1=0.1$ mb., without altering any listed value in the radiosoundings of their Appendix A.

The WYL computation of the atmospheric transmissivity from the ith layer below the top is in general based upon "universal" transmission functions, after Cowling [1], with appropriate values of $(l,u/2)$ and of the *effective* dimensionless pressure parameter P_e defined as

$$P_e(u_i)=\left(\int_0^{u_i} p\, du\right)\Big/ p_0 u_i. \qquad (2)$$

Here u_i is the optical path of the particular radiative constituent from level 1 to level i. The parameter $P_e(u_N)$ of (2) is used in connection with our statistical tests of section 5. The curves of figures 1, 3, and 5 of WYL [13] show graphically the nature of the transmission curves used in the various wave band intervals, excluding the water vapor window contribution (for the latter, see figure 4 of WYL [13]). In addition to the transmissivity, the other major parameter for determining the band transmittance from the ith layer is the black body (Planckian) intensity function

$$I_{B\nu}=c_1\nu^3/[\exp\,(c_2\nu/T)-1] \tag{3}$$

where the constants c_1, c_2 have the values

$$c_1=1.190\times10^{-12}\text{ watts cm.}^2\text{ (ster.)}^{-1}$$

$$c_2=1.4389\text{ cm. °K.}$$

The WYL summations of $\Sigma I_\nu(\theta)\Delta\nu$ over each of the 77 band intervals spanning the terrestrial spectrum gives the "top of the atmosphere" intensity $I(\theta)$ at zenith angle θ. These resulting intensities $I(\theta)$ were listed by WYL [13] in their Appendix B for each model atmosphere and each of the five angles previous noted. Values of the filtered radiances as computed for the channels 2 and 4 scanning radiometers of TIROS 1, 2, and 4, where applicable, were also listed in the WYL Appendix B.

In 1966, after making use of the effective response functions of the NIMBUS II medium resolution infrared radiometers ([10], chap. 4), Wark et al. computed revised values of the filtered radiances for the newly designed channels 2 and 4, now encompassing the 10–11 and 5–30 micron regions, respectively. Wark et al.[3] kindly made these revised 1966 radiances available to the authors, along with minor revisions in the unfiltered emergent intensities $I(\theta)$, resulting from minor improvements in the 1966 version of the WYL radiative transfer model. These revised (1966) intensities, $I(\theta)$, were therefore employed in the computation of F_{WYL} by equation (1).

The use of the EC model suggested itself to the authors in view of the relative simplicity of application of its radiative tables to the operational radiosounding. Any sounding subjected to this model should, however, be extended to the 0.1-mb. level by use of an appropriate Supplementary Standard Atmosphere [11]. Another simplifying difference, which suggested an experimental use of the EC model, lies in the system of pressure scaling used in accounting for the Lorentz line width broadening. The EC model incorporates a linear pressure-scaling factor, layer by layer, into an effective path u_j^* at the jth level, ($j=1, \ldots, N$), involving only j-summations over the reduced optical mass to the jth level of the sounding. With the WYL model, a twofold summation process is required: one involving optical mass and the other involving the effective pressure, $P_e(u_j)$. In this latter model, the number of summation iterations required to specify the transmissivities along the sounding path is essentially doubled.

Besides the major computational differences just cited, a number of minor differences in the models exist. The values of the generalized absorption coefficients differ slightly from one model to the other. Also, the WYL model spans the terrestrial spectrum by 77 spectral intervals, whereas the EC model uses 60 divisions each of 40 cm.$^{-1}$ in accomplishing this purpose.

[3] Private communication.

Obviously the restriction in vertical resolution in adapting the EC model directly to the radiosoundings of the WYL model atmospheres ([13], Appendix A), as well as the comparative simplicity in expressing line width broadening effects may both adversely affect the comparison of the computed fluxes. On the other hand, a consistent and predictable difference flux residual, $F_{WYL}-F$, could result from the study. This would be a useful byproduct of the study.

2. THE DATA REDUCTION

All 63 radiosoundings tested by the EC method of flux computation had a format similar in general to that of table 1 (drawn directly from case 3 in Appendix A of [13]), which depicts a clear-sky radiosounding for Oakland, Calif., taken at 1200 GMT, Sept. 29, 1958. All 51 cases in the numbered sequence 50 to 100 of the Appendix A [13] are used in similar format. Of these soundings, 49 have black body cloud-top interfaces at levels designated in Appendix A. Apart from these overcast situations, 14 clear-sky soundings have been selected randomly from the same source. In processing each sounding for adaptation to the EC model, the level $p=0.1$ mb. in the last line of table 1 is taken as level 1, while the interface level listed first is taken as level N (see fig. 1), regardless of the nature of the interface, cloud-top or earth-surface.

The number N varied generally in the range 20 to 30. The specific set of soundings actually used are identified in table 2, column one, each sounding having the listed number given it in Appendix A of WYL [13].

The EC computational scheme depends upon the precalculated emission tables $R(u^*,T)$ listed in chapter VI of Elsasser and Culbertson [2] (pp. 36–45). For entry into these tables, one needs the reduced optical paths for each of the three constituents, water vapor, carbon dioxide, and ozone at the $(j+1)$th level, i.e., j levels below $p_1=0.1$ mb. These three optical paths will be denoted,

TABLE 1.—*A typical example of a sounding in the WYL Appendix* [13]

Case	Level	Temp. (°K.)	Pressure	H_2O (gm./kg.)	Ozone S.T.P. cm. $\times$ 10^{-5} (mb.)$^{-1}$
3	28	289	1009.0000	9.4000	0
	27	288	1000.0000	9.4000	0
	26	293	997.0000	8.9000	0
	25	301	906.0000	6.9000	.300
	24	295	850.0000	5.2000	.500
	23	265	500.0000	1.6000	2.500
	22	252	400.0000	.3000	4.000
	21	224	250.0000	.0320	8.000
	20	218	228.0000	.0210	10.000
	19	210	185.0000	.0080	14.000
	18	212	150.0000	.0140	20.500
	17	206	100.0000	.0110	42.000
	16	205	93.0000	.0120	47.500
	15	212	50.0000	.0220	131.000
	14	222	25.0000	.0450	330.000
	13	225	15.0000	.0750	460.000
	12	226	12.0000	.0940	492.500
	11	230	10.0000	.1120	513.000
	10	241	6.0000	.1120	563.500
	9	249	4.0000	.1120	642.500
	8	256	3.0000	.1120	623.000
	7	265	2.0000	.1120	547.500
	6	283	1.0000	.1120	255.000
	5	283	.6000	.1120	25.500
	4	271	.4000	.1120	2.500
	3	262	.3000	.1120	1.500
	2	251	.2000	.1120	.500
	1	231	.1000	.1120	.100

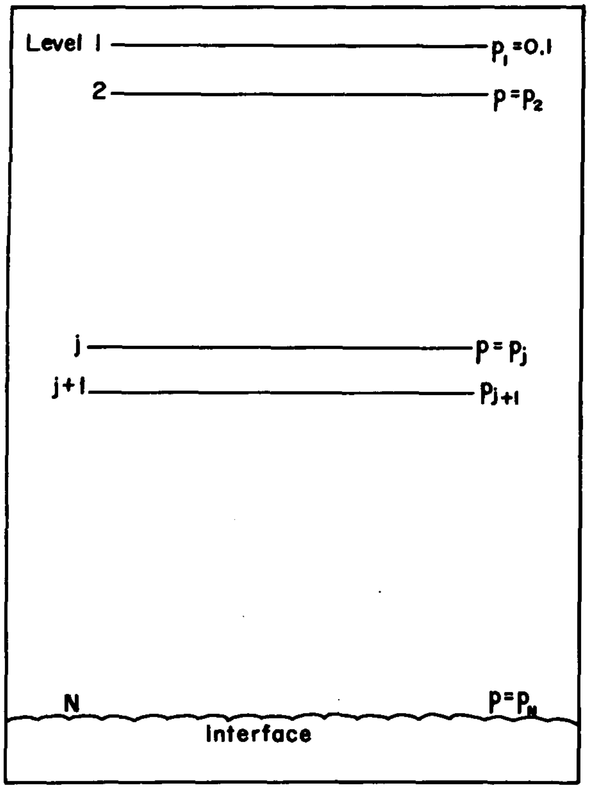

FIGURE 1.—Sounding-level designation for the computation of upward flux through level 1, where $p_1=0.1$ mb. The reduced depth is integrated downward to level N, which is taken to be a black body interface.

respectively by u^*_{j+1}=the reduced optical mass of water vapor from $p_1=0.1$ mb. to $p_{j+1}(j=1, \ldots, N-1)$; $\mathcal{U}^*_{j+1}$, the same as u^*_{j+1} but in reference to carbon dioxide; U^*_{j+1}, the same as u^*_{j+1}, but in reference to ozone (fig. 1).

The three different forms of the letter u, are to be observed carefully for reference to the radiating agent under discussion. While the three forms are distinctively different, they still suggest their use in connection with the R-function tables of Elsasser and Culbertson [2] (especially the EC tables 18, 11, 13, respectively, and our adaptation of these tables to shorter optical paths).

The Elsasser-Culbertson method for describing the averaged pressure broadening along a ray path involves the parameter u^*_{j+1} (for water vapor), which is defined first in terms of the element of optical path

$$du=\frac{1}{g}\,q\,dp \qquad (4)$$

and then by the linearly scaled pressure integral of (4)

$$u^*_{j+1}=\int_{p=0.1}^{p_{j+1}}\left(\frac{p}{p_0}\right)du. \qquad (5)$$

In (4), q is the mixing ratio of water vapor (listed for each case in the second last column of the table 1 format), g=980 cm. sec.$^{-2}$, p is the pressure, and p_0=1013.25 mb. When (5) is integrated in the sense of increasing p using the trapezoidal approximation for finite layers, one obtains the result

$$u^*_{j+1}=2.5177\times10^{-7}\sum_{i=1}^{j}(q_{i+1}+q_i)(p^2_{i+1}-p^2_i),$$
$$j=1, \ldots, N-1, \qquad (6)$$

with the result in gm. cm.$^{-2}$ of water vapor.

In formulating the analog for $\mathcal{U}^*_{j+1}$, it is necessary to recall that path is to be pressure weighted as in the integral form (5), but du must be replaced by the S.T.P. depth of thickness dz. Thus the reduced S.T.P. path element of carbon dioxide becomes

$$d\mathcal{U}^*=(3.14\times10^{-4})\left(\frac{p}{p_0}\right)^2\frac{T_0}{T}dz$$

where 3.14×10^{-4} is the proportion by volume of this particular gas. Integration of $\mathcal{U}^*$ over j successive layers of a sounding leads (see Martin and Palmer [8]) to the result in S.T.P. cm.

$$\mathcal{U}^*_{j+1}=\frac{3.14\times10^{-1}}{2g\rho_0p_0}\sum_{i=1}^{j}(p^2_{i+1}-p^2_i). \qquad (7)$$

In (7), all pressures are in mb.; then with the standard values $g\rho_0$=1.20131 gm. cm.$^{-2}$ sec.$^{-2}$ and p_0=1013.25 mb., one obtains

$$\mathcal{U}^*_{j+1}=1.28985\times10^{-5}\sum_{i=1}^{j}(p^2_{i+1}-p^2_i),$$
$$j=1, \ldots, N-1. \qquad (8)$$

The final column of table 1 indicates that the ozone mixing ratio is already in S.T.P. cm.(mb.)$^{-1}$, so that the column depths of ozone have only to be pressure corrected in a manner similar to (5) where this is empirically applicable. Elsasser and Culbertson [2] interpret Walshaw's [12] measurements to indicate that a linearly scaled pressure factor of the type used in (5) is applicable for $p/p_0\leq$ 0.1316. For higher pressures, the pressure-broadening effect is taken as limited by this constant pressure ratio. The integration for U^* proceeds in a manner analogous to (1) and (5) with q_i replaced by Q_i, and becomes

$$U^*_{j+1}=2.4673\times10^{-9}\sum_{i=1}^{j}(Q_{i+1}+Q_i)(p^2_{i+1}-p^2_i),$$
$$j=1, \ldots, j\leq j_c \qquad (9)$$

for $(p_{j+1}+p_j)/2\ \leq\ p_c$=133.2 mb. For integrations extending below this level, U^*_{j+1} consists of a part identical to (9) extending to the level p_{j_c} *closest to but above* p_c, supplemented by the additional contribution from layers having mean pressures $\bar{p}_j\geq p_{j_c}$. This additional contribution from layers of mean pressure higher than p_{j_c}, has the form

$$\Delta U^*(j_c, j+1)=6.55789\times10^{-7}\sum_{i=j_c}^{i=j}(Q_{i+1}+Q_i)(p_{i+1}-p_i),$$
$$j=j_c, \ldots, N-1. \qquad (10)$$

For ozone U^*_{j+1}, in reduced S.T.P. cm., is given either by (9), or by (9) supplemented by (10) when $\bar{p}_j\geq$133.2 mb.

TABLE 2.—*Listing of contributions to emergent flux at the top of the atmosphere made by adapting the Elsasser-Culbertson [2] radiative transfer model to the indicated sounding case from the WYL model atmospheres [13]*

Case Number	F_W	DFCO2	F'_C	DFO3	F'_O	Total flux from air	τ_F(Net)	Interface flux transmission	Total flux at top
2	160.566	23.514	7.594	2.578	0.200	168.361	0.06224	26.003	194.364
3	167.282	24.630	6.522	2.576	0.003	173.807	0.07006	27.704	201.511
4	127.821	14.624	15.931	1.135	1.679	145.431	0.14849	54.759	200.190
7	107.956	8.031	20.451	0.506	2.425	130.652	0.25458	73.342	203.994
8	92.385	4.682	23.092	0.249	2.200	117.677	0.33891	90.526	208.203
10	188.630	27.612	3.436	4.197	1.312	193.379	0.03482	15.568	208.947
12	124.422	12.336	16.718	1.009	2.148	143.288	0.18014	64.588	207.876
13	118.032	11.147	18.477	0.852	2.407	138.916	0.18760	63.517	202.433
20	133.291	14.138	14.145	1.180	1.569	149.005	0.17383	70.661	219.666
23	98.515	6.574	22.244	0.468	2.996	123.755	0.28935	92.451	216.206
27	93.878	4.821	22.284	0.294	2.516	118.678	0.34416	86.441	205.119
31	66.097	0.909	23.119	0.045	2.385	091.601	0.55932	96.697	188.298
50	98.981	4.502	25.221	0.294	4.166	122.368	0.36546	118.482	240.850
51	76.158	1.427	28.147	0.093	4.510	108.815	0.53962	157.803	266.618
52	68.097	0.758	22.623	0.053	3.375	094.095	0.61558	161.930	256.025
53	91.606	3.762	25.510	0.250	3.091	119.207	0.39605	128.400	247.607
54	77.987	2.160	16.622	0.136	1.482	096.091	0.46136	127.041	223.132
55	141.934	15.355	15.654	1.302	2.035	159.623	0.15397	57.582	217.205
56	50.605	0.234	16.627	0.014	1.682	068.914	0.74774	162.942	231.856
57	66.009	1.029	26.078	0.064	3.331	095.419	0.54460	80.538	175.957
58	59.343	0.488	16.711	0.032	1.967	078.021	0.65131	161.465	239.486
59	154.839	20.052	8.516	2.263	0.681	164.036	0.08306	33.763	197.799
60	67.890	0.919	21.731	0.064	3.176	092.797	0.58092	152.813	245.610
61	117.817	9.439	15.349	0.774	1.834	135.000	0.23102	84.001	219.001
62	90.997	3.260	20.336	0.229	2.402	113.735	0.40615	129.768	243.503
63	103.576	5.430	21.315	0.380	2.743	127.634	0.34900	126.897	254.531
64	30.158	0.018	19.003	0.001	2.685	051.846	0.90988	144.338	196.184
65	87.144	4.607	19.539	0.327	2.568	109.250	0.33375	96.151	205.401
66	87.536	3.933	20.333	0.274	2.631	110.502	0.36417	103.350	213.852
67	67.410	1.031	21.483	0.074	2.889	093.782	0.56226	147.930	241.712
68	42.171	0.090	20.568	0.006	2.940	065.679	0.81483	148.204	213.883
69	57.291	0.471	22.887	0.032	2.925	083.103	0.65666	140.809	223.912
70	58.889	0.512	22.782	0.036	2.857	084.528	0.64883	143.672	228.200
71	72.879	1.282	19.793	0.081	2.398	095.070	0.52853	145.536	240.606
72	70.238	0.844	21.006	0.052	2.730	093.974	0.60259	168.456	262.430
73	110.212	9.324	15.830	0.666	1.802	127.844	0.22136	77.128	187.340
74	136.376	15.289	14.074	1.306	0.719	152.169	0.13163	49.231	201.400
75	143.181	15.724	16.018	1.293	1.948	161.147	0.14261	56.932	218.079
76	128.582	14.126	17.438	1.105	2.135	148.155	0.14319	47.101	195.256
77	64.554	0.557	25.210	0.034	3.702	093.466	0.64189	156.381	249.847
78	59.423	0.430	23.232	0.025	3.164	085.825	0.67475	156.713	242.538
79	48.619	0.153	22.317	0.009	3.245	074.183	0.77058	154.833	229.016
80	93.147	4.342	27.916	0.244	3.979	125.042	0.35202	102.942	227.984
81	45.813	0.114	21.574	0.007	3.126	070.512	0.80129	155.788	226.300
82	37.666	0.045	19.948	0.002	2.508	060.122	0.85850	143.432	203.554
83	84.352	3.011	22.570	0.193	2.453	109.375	0.40657	111.954	221.329
84	77.698	1.896	23.318	0.122	2.780	103.797	0.47837	137.739	241.536
85	85.080	3.314	21.817	0.193	2.440	109.337	0.38971	110.599	219.936
86	56.059	0.508	20.734	0.030	2.283	079.076	0.64744	138.832	217.908
87	17.104	0.002	14.072	0.000	1.514	032.690	0.96056	129.891	162.581
88	56.623	0.451	20.419	0.024	1.927	078.969	0.67588	144.931	223.900
89	50.530	0.168	22.793	0.010	3.240	076.562	0.76765	159.363	235.925
90	45.174	0.086	19.755	0.006	3.006	067.935	0.83760	186.209	254.144
91	173.965	25.278	6.832	0.927	0.865	180.932	0.05866	26.934	207.866
92	120.384	10.037	15.700	0.769	1.985	138.069	0.22214	81.918	219.987
93	115.276	9.103	16.929	0.654	1.907	134.112	0.23656	86.013	220.125
94	143.331	16.492	11.456	1.566	1.203	155.990	0.12917	51.079	207.069
95	111.993	8.176	16.211	0.649	1.870	130.074	0.24569	83.186	213.260
96	73.603	1.453	25.975	0.104	2.874	102.452	0.54331	203.194	305.646
97	130.259	12.894	14.957	1.034	1.750	146.966	0.17110	61.338	208.304
98	94.529	3.816	24.654	0.231	3.190	122.373	0.38318	120.654	243.027
99	98.050	5.156	22.428	0.333	2.430	122.917	0.34702	106.099	229.016
100	68.273	1.111	24.222	0.075	3.340	095.835	0.54771	131.280	227.115

In numerical computation of the radiative transfer by the EC model, the sounding is transformed to a set of values $(u_j^*, \mathcal{U}_j^*, U_j^*, T_j)$ now known at each level j by equations (6), (8), (9), and (10), for each of the three constituents. The sounding is further transformed into an $R_j[u^*(T_j), T_j]$ distribution extending from the reference level to the interface. The EC definition of $R(u^*,T)$ is given by equation (80) of [2] (p. 32),

$$R(u^*, T)=\int_{\nu_1}^{\nu_2}\pi\frac{dI_{B\nu}}{dT}[1-\tau_{F\nu}(u^*)]d\nu, \tag{11}$$

for the particular constituent u^* under consideration. Numerical values of $R(u^*, T)$ are listed for water vapor, ozone, and carbon dioxide, respectively, in EC tables 18, 13, and 11 in terms of a linear scale of temperature and of a logarithmic scale of reduced optical path. These numerical $R(u^*, T)$ tables are listed as a part of our *main* computational program, together with a linear interpolation subroutine upon the two coordinate axes so that a value of $R(u_j^*, T_j)$ can be determined for each constituent and any sounding level (see fig. 2).

The particular tables just referred to have lower limits u_f^* of reduced optical paths of 10^{-5} gm. cm.$^{-2}$ for water vapor, and of 10^{-4} cm. S.T.P. for both ozone and carbon

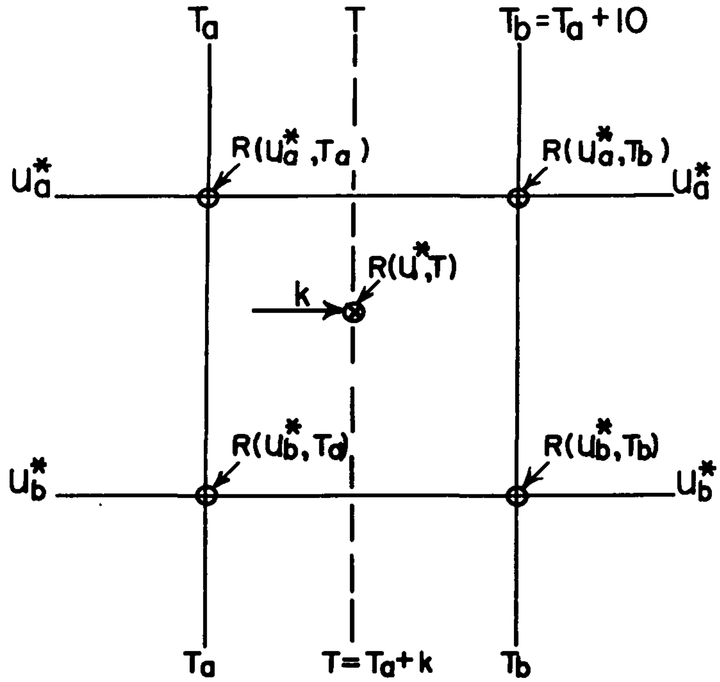

FIGURE 2.—Schematic illustration of the interpolation for $R(u^*, T)$ when a point (u^*, T) does not coincide with an entry value in the Elsasser-Culbertson tables. The values of u^*_a, u^*_b, and u^* are actually represented on a logarithmic scale, and the u^*-interpolation is logarithmic. The temperature scale is linear (in degrees Celsius).

dioxide. It was therefore found necessary to include an algorithm for extension of these EC tables to values of u^*, U^*, $\mathcal{U}^*$ several orders of magnitude lower than the minimum listed tabular value $u^*_f=10^{-n_1}$ for the three constituents.

The flux transmissivity functions employed by Elsasser and Culbertson are based upon their equations (35) and (27) ([2], pp. 6–7), the former equation for water vapor and ozone, the latter for the more regular carbon dioxide band. These transmissivity functions, after EC, may be taken as:

$$\tau^w_{F\nu}= \exp\left[-\left(\frac{5}{3}l_\nu u^*\right)^{1/2}\right]$$

$$\tau^o_{F\nu}= \exp\left[-\left(\frac{5}{3}L_\nu U^*\right)^{1/2}\right]$$

$$\tau^c_{F\nu}=1- \operatorname{erf}\left(\frac{5}{3}\mathcal{L}_\nu\,\mathcal{U}^*\right)^{1/2}. \tag{12}$$

Here ν indicates an average over a limited interval $\Delta\nu$ centered at ν; l_ν, L_ν, $\mathcal{L}_\nu$ are the *generalized absorption coefficients* for the indicated constituent water vapor, ozone, and carbon dioxide, respectively, and are listed by wave interval span in EC tables 10, 9, and 8. Even for the largest l_ν, L_ν, $\mathcal{L}_\nu$ values listed in these tables, the function $1-\tau_{F\nu}$ of the right side of (11) was already closely approximated by the square root of u^*. Thus for any temperature T, the extension of the EC tables 18, 13, and 11 has been programmed as an adjunct to these tables in the manner displayed above for $u^*<u^*_f$.

	$R_w(u^*, T)$	$R_o(U^*, T)$	$R_c(\mathcal{U}^*, T)$
$u^*_f=10^{-n_1}$	$R_w(-n_1, T)$	$R_o(-n_1, T)$	$R_c(-n_1, T)$
$u^*=10^{-n_1-.3}$	$(.5)^{1/2}R_w(-n_1, T)$	$(.5)^{1/2}R_o(-n_1, T)$	$(.5)^{1/2}R_c(-n_1, T)$
$u^*=10^{-n_1-.7}$	$(.2)^{1/2}R_w(-n_1, T)$	$(.2)^{1/2}R_o(-n_1, T)$	$(.2)^{1/2}R_c(-n_1, T)$
$u^*=10^{-n_1-1.0}$	$(.1)^{1/2}R_w(-n_1, T)$	$(.1)^{1/2}R_o(-n_1, T)$	$(.1)^{1/2}R_c(-n_1, T)$

This procedure was extended to values of u^* as small as required. Henceforth the EC tables 18, 13, and 11 are understood to be the extended tables, illustrated in the tabular form just shown. With the use of these extended $R(u^*, T)$ tables, the data processing was completed when the values

$$R(u^*_1, T_1)R(u^*_2, T_2), \ldots, R(u^*_N, T_N)$$

were computed for each constituent and each sounding level, as well as for all soundings considered.

It is convenient, in passing, to discuss the transmissivity functions a little further. The first two of (12) are based upon the Goody [3] statistical band model, while the third formula in (12) is based upon the fact that carbon dioxide band has a regular, periodic line structure appropriate to Elsasser band transmission [2]. In all three forms of (12), line width is assumed small relative to line spacing. All generalized absorption coefficients l_ν, although reduced to standard laboratory conditions ($p=p_0$, $T=293$°K.), are considered by EC to be independent of temperature.[4] In addition, beam transmissivities are considered converted to flux transmissivities by use of the multiplicative factor 5/3 associated with each u^* in (12). Finally in any spectral region $\Delta\nu$ where two constituents absorb and emit jointly, the resultant transmissivity is assumed to be given by the produce-transmissivity approximation

$$\tau^{wc}_{F\nu}=\tau^w_{F\nu}\tau^c_{F\nu} \tag{13}$$

using water vapor and carbon dioxide as examples.

3. THE RADIATIVE MODEL

This section will be divided into three parts. In the first subsection, each of the three constituents will be considered within its appropriate spectral limits, as if there were no regions of overlap with other constituents. In the second subsection, atmospheric overlap effects are considered. In the third subsection, interface emission and subsequent transmission by the atmosphere are introduced.

ATMOSPHERIC COMPUTATIONS ASSUMING NO OVERLAP

Here the discussion of any one constituent will be representative also of the other two constituents provided the proper $R(u^*, T)$ table is employed. In terms of the R-function (11), the single constituent flux through the level 1 (fig. 1) may be written in the form

$$F=\int_{T_N}^{T_1} R[u^*(T), T]dT+\int_{-273}^{T_N} R[u^*_N, T]dT \tag{14}$$

[4] In most of the recent radiative models, e.g., WYL [13] and others, the generalized absorption coefficient for carbon dioxide is considered temperature dependent. The $\mathcal{L}_\nu$ values of EC are based upon both temperature and path averaging to give values most nearly representative of the upper troposphere ([2], pp. 18-19).

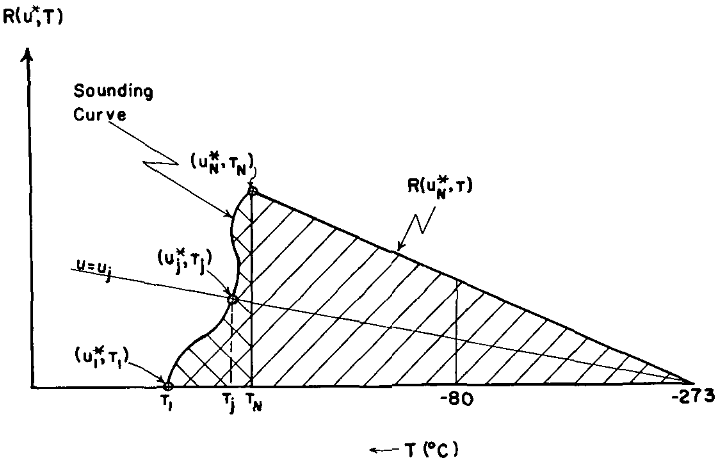

FIGURE 3.—Schematic depiction of an atmospheric sounding $u^*=u^*(T)$ in coordinates of $R(u^*, T)$ and T. The reference level is represented by (u^*_1, T_1), and the final, interface level by (u^*_N, T_N). The ordinate $R(u^*, T)$ is the appropriate Elsasser-Culbertson [2] tabular value listing for the single constituent under consideration. The flux from the atmospheric constituent is represented by combined hatched areas.

which is a direct application of the flux equation (83) of EC. Numerical integration of (14) is conveniently carried out using the trapezoidal approximation, and leads to result

$$F=\sum_{i=N-1}^{i=1}\left[\frac{R_i(u_i^*, T_i)+R_{i+1}(u^*_{i+1}, T_{i+1})}{2}\right](T_i-T_{i+1})$$
$$+\sum_{j=0}^{i=k}\left[\frac{R(u_N^*, T_{N+j})+R(u_N^*, T_{N+j+1})}{2}\right](T_{N+j}-T_{N+j+1})$$
$$+\int_{-273}^{-80}R(u_N^*, T)\,dT. \qquad (15)$$

In (15), T_{N+k} represents the kth multiple of 10°C. in the direction T_N towards −80°C. For example,[5] with T_N in degrees Celsius,

$$T_{N+1}=10[T_N/10],\ T_{N+2}=T_{N+1}-10,\ \ldots,\ T_{N+k+1}=-80°C.$$

The integral F of (15) is depicted schematically by the combined hatched areas of figure 3. The first summation in (15) is represented by the doubly hatched area on the left. The second summation is the singly hatched area between T_N and −80°C. The final integral in (15) corresponds to the "triangular" segment beneath $R(u_N^*, T)$ from −80°C. to the apex at −273.16°C., and has listed values for each constituent in EC table 20. The EC table is not included here but has been included in the main computer program.

It is convenient to simplify the notation when dealing with the flux integral in the form (14). The two integrals of (14) may be *formally* combined as

$$F=\int_{T=0}^{T_1}R(u^*, T)dT \qquad (16)$$

with the understanding that the integration must, in fact, consist of the *two parts*, depicted respectively by the singly and doubly hatched portions of figure 3. Note also that the temperature limits on the integration have been converted to degrees Kelvin. However $R(u^*, T)$ is still determined using EC tables 18, 13, and 11, which list T in degrees Celsius.

At this point in the program, we have used equation (15) to compute separate flux contributions F_w, F_c, and F_o due to water vapor, carbon dioxide, and ozone, with no overlap corrections. The three types of computations made involve flux transmission in the spectral ranges:

a) 20 to 2420 cm.$^{-1}$ for water vapor using EC table 18,

b) 540 to 820 cm.$^{-1}$ for carbon dioxide using EC table 11,

c) 970 to 1130 cm.$^{-1}$ for ozone using EC table 13.

The resulting computations of F_w are to be found in column 2 of table 2 for each sounding; F_c must be obtained as the sum of the adjacent column 3 and 4 entries. F_o is the sum of column entries 5 and 6 for each case. All fluxes listed in table 2 have been converted to units of watts m.$^{-2}$ The remaining columns of table 2 are to be described in the next two subsections, as well as the reason for the decomposition of F_c into the two parts DFCO2 and F_c', etc.

OVERLAP CORRECTIONS IN ATMOSPHERIC FLUX COMPUTATIONS

The radiative transfer effected by atmospheric carbon dioxide and ozone are now corrected for overlap with water vapor in the spectral regions (b) and (c) listed at the end of the preceding subsection. In the region (c), the primary absorber is ozone, and here water vapor has only a weak continuous absorption spectrum. Ozone also has an absorption band near 14 microns, but with generalized absorption coefficients generally between 2–3 orders of magnitude smaller than those of water vapor in the region 540–820 cm.$^{-1}$ As a result, ozone overlap has been neglected in region (b).

When the combined outgoing flux due to water vapor and carbon dioxide is formulated in the overlap region (b), with $\tau_{F\nu}^{wc}$ of (13) inserted into (11) and (15), an enhanced mean slab absorptivity for the overlapped band interval results. The resultant two-constituent flux, here denoted F_{wc}, may be written in the compact integral form of equation (16), as

$$F_{wc}=F_w''+\int_0^{T_1}\left\{\int_{\nu_1}^{\nu_2}\pi\frac{dI_{B\nu}}{dT}[1-\tau_{F\nu}(u^*)\tau_{F\nu}(\mathcal{U}^*)]d\nu\right\}dT. \qquad (17)$$

Here F_w'' is the water vapor flux excluding *any contribution in the interval* ν_1 to ν_2 (540–820 cm.$^{-1}$). If this latter contribution, F_w-F_w'', of the deleted water vapor flux is now added and subtracted to the right side of (17), one readily obtains the equivalent expression for F_{wc}

$$F_{wc}=F_w+\int_0^{T_1}\left\{\bar{\tau}_F(u^*)\int_{\nu_1}^{\nu_2}\pi\frac{dI_{B\nu}}{dT}[1-\tau_{F\nu}(\mathcal{U}^*)]d\nu\right\}dT \qquad (18)$$

where $\bar{\tau}_F(u^*)$ is the slab transmissivity for a water vapor

[5] The notation $[x]$ is the integral part of the value x, which may be a positive or negative decimal number.

308-679 O - 68 - 3

TABLE 3.—Mean water vapor flux emissivity $\bar{\epsilon}_F(u^*)$ computed from equation (19) as a function of u^* for the water vapor carbon dioxide overlap region (540–820 cm.$^{-1}$)

$\log u^*$	$\bar{\epsilon}_F(u^*)$	$\log u^*$	$\bar{\epsilon}_F(u^*)$
−6.3	.000240	−2.7	.014488
−6.0	.000339	−2.3	.022719
−5.7	.000480	−2.0	.031916
−5.3	.000759	−1.7	.049395
−5.0	.001074	−1.3	.068445
−4.7	.001518	−1.0	.094068
−4.3	.002400	−0.7	.127928
−4.0	.003395	−0.3	.187784
−3.7	.004801	−0.0	.245327
−3.3	.007165	0.3	.313624
−3.0	.010230	0.7	.415446

reduced path u^*, averaged over the 540–820-cm.$^{-1}$ interval. Values of $\bar{\tau}_F(u^*)$ for water vapor in the 540–820-cm.$^{-1}$ interval may be inferred from table 3, using $\bar{\tau}_F=1-\bar{\epsilon}_F(u^*)$. The $\bar{\epsilon}_F$ values of table 3 are approximated using equation 6.46 of Goody [4] with $\epsilon_{F\nu}(u^*)$ introduced from (12). The resultant computational formula for $\bar{\epsilon}_F(u^*)$ is

$$\bar{\epsilon}_F(u^*)=\sum_i\left[1-\exp\left(-\frac{5}{3}\,l_{\nu i}u^*\right)^{\frac{1}{2}}\right](\pi dI_{B\nu}/dT)_i\Big/\sum_i\left(\pi\frac{dI_{B\nu}}{dT}\right)_i. \tag{19}$$

Here the index i spans the range 560–800 cm.$^{-1}$, inclusive, by 40-cm.$^{-1}$ intervals. As previously noted, equation (19) and the resultant table 3 have been treated assuming that the l_ν values of EC table 10 are dependent of temperature ($T=293$°K.).

The substitution $\bar{\tau}_F(u^*)=1-\bar{\epsilon}_F(u^*)$ made in (18) leads to a form of the two-constituent flux stream

$$F_{wc}=F_w+F_c-\int_0^{T_1}\bar{\epsilon}_F(u^*)R_c(\mathcal{U}^*,\ T)dT \tag{20}$$

which is useful for interpretation. Equation (20) affords insight concerning the disposition of the "overlapped carbon dioxide flux," represented by the last term of (20). This term has been denoted DFCO2

$$\text{DFCO2}=\int_0^{T_1}\bar{\epsilon}_F(u^*)R_c(\mathcal{U}^*,\ T)dT. \tag{21}$$

On the other hand, the net carbon dioxide flux F_c' transmitted from the atmosphere is the residual of the last two terms of (20).

In order to simplify the computation of DFCO2, it is desirable to retain in computer memory each term in the summation (15) which led to F_c. One then simply multiplies the ith term in the first summation of (15) by

$$\bar{\epsilon}_F(u^*_{i-1}),\qquad i=1,\ .\ .\ .,\ N-1$$

and the final two sets of summations in (15) by $\bar{\epsilon}_F(u^*_N)$.

The two-constituent flux arising from an atmosphere of water vapor and ozone with overlap in the 970–1130-cm.$^{-1}$ interval is obtained by analogy with F_{wc} of (18) as

$$F_{wo}=F_w+\int_0^{T_1}\bar{\bar{\tau}}_F(u^*)R_o(U^*,\ T)dT \tag{22}$$

where $R_o(U_i^*,\ T_i)$ comprises the complete set of stored R_o-values for the sounding determined as described in section 2. In (22), $\bar{\bar{\tau}}_F(u^*)$ is mean slab transmissivity of u^* gm. cm.$^{-2}$ of water vapor in the spectral region 970–1130 cm.$^{-1}$ The computation of $\bar{\bar{\tau}}_F(u^*)$ has been modeled after the procedure of Hanel, Bandeen, and Conrath [5], treating water vapor as a weak continuum of absorption in the interval under discussion. A water vapor beam transmissivity of form $\exp(-ku^*)$, and a corresponding slab transmissivity

$$\bar{\bar{\tau}}_F(u^*)=\exp\left[-\frac{5}{3}ku^*\right]=\exp\left(-0.1167u^*\right) \tag{23}$$

has been selected with the value of k identical to that of Hanel et al. [5]. If we write $\bar{\bar{\tau}}_F=1-\bar{\bar{\epsilon}}_F(u^*)$, we obtain F_{wo} in a form analogous to that of F_{wc} of (20), with the overlapped ozone flux given by

$$\text{DFO3}=\int_0^{T_1}\bar{\bar{\epsilon}}_F(u^*)\ R_o(U^*,\ T)dT. \tag{24}$$

The computation of (24) is facilitated by the procedure described in the paragraph immediately below (21).

The residual or nonoverlapped flux in this interval, denoted F_o', is then simply

$$F_o'=F_o-\text{DFO3}.$$

For the three-constituent atmosphere, with overlap regions (b) and (c) as described below equation (16), we obtain the total emergent atmospheric flux as

$$F_{atr}=F_w+F_c'+F_o'. \tag{25}$$

In arriving at this result, we have considered water vapor as depleting the carbon dioxide and ozone radiative streams, rather than the reverse type of overlap consideration. A more realistic partition of the three emergent flux contributions would presumably be given by the expressions listed below

$$\hat{F}_w=F_w-(\text{DFCO2})/2-(\text{DFO3})/2$$

$$\hat{F}_c=F_c'+(\text{DFCO2})/2$$

$$\hat{F}_o=F_o'+(\text{DFO3})/2$$

without altering the total outgoing flux (25) from the atmosphere.

INTERFACE CONTRIBUTIONS TO THE EMERGENT FLUX

The interface in all of the model atmospheres studied here is considered a black body either at the earth's surface or at the top of a dense undercast with temperature T_N. In either case there is a variable number N of sounding levels above the interface, and an atmosphere containing total reduced optical depths u_N^*, $\mathcal{U}_N^*$, U_N^* of the three radiating constituents between the interface and the top of the atmosphere (at $p_1=0.1$ mb.), where $u_1^*=\mathcal{U}_1^*=U^*=0$.

The flux originating at the interface is the familiar integral of the Planck function (equation (3))

$$F_B=\int_{\nu_1=20}^{\nu_2=2420}\pi I_{B\nu}(\nu,\ T_N)d\nu=\sigma T_N^4 \tag{26}$$

where

$$\sigma=5.6687\times10^{-8}\text{ watt m.}^{-2}\text{ °K.}^{-4}$$

Within the spectral range of integration indicated in (26), the slab transmissivities of the overlying water

TABLE 4.—*Fractions $c_1(T_N)$ and $c_2(T_N)$ of black body flux contained within the carbon dioxide and ozone band intervals*

	540–820 cm.$^{-1}$	970–1130 cm.$^{-1}$
T_N(°K.)	$c_1(T_N)$	$c_2(T_N)$
313.16	.27255	.10318
303.16	.27883	.10004
293.16	.28457	.096623
283.16	.28963	.092527
273.16	.29390	.088004
263.16	.29707	.082753
253.16	.298964	.077116
243.16	.298956	.071002
233.16	.29794	.064413
223.16	.29444	.057607

vapor, carbon dioxide, and ozone are listed individually in the EC tables 7, 3, and 5 respectively. We label the full atmospheric depth transmissivities for the three constituents simply by $\tau_F(u_N^*)$ for water vapor, $\tau_F(\mathcal{U}_N^*)$ for carbon dioxide, and $\tau_F(U_N^*)$ for ozone. The contents of EC tables 7, 3, and 5 provide values for these individual transmissivities. These tables are not reproduced here but have been added, however, as part of the computational program.

It should be noted that $\tau_F(u_N^*)$ now spans the entire spectrum, whereas $\tau_F(\mathcal{U}_N^*)$ has been modeled to span the interval 540–820 cm.$^{-1}$, within which interval there is only a fraction $c_1(T_N)$ of the surface black body flux σT_N^4. Likewise $\tau_F(U_N^*)$ essentially spans only the interval 970–1130 cm.$^{-1}$, where there is only a fraction $c_2(T_N)$ of the interface flux σT_N^4. The fractions $c_1(T_N)$, $c_2(T_N)$ are now to be determined.

If the Planck function, equation (3), is transformed into its nondimensional form ([2], p. 3)

$$\int_{\nu_1}^{\nu_2} \pi I_{B\nu}(\nu, T_N) d\nu = \sigma T_N^4 \left(\frac{1}{6.4939} \int_{x_1}^{x_2} \frac{x^3}{(e^x-1)} dx \right) \quad (27)$$

with $x=(1.4389\nu)/T_N$, the fractions $c_1(T_N)$ and $c_2(T_N)$ become the multipliers of σT_N^4 in (27). Of course appropriate limits are to be assigned for x_1 and x_2. A tabular set of values $c_1(T_N)$, $c_2(T_N)$, has been obtained by integration of (27), using limits $(\nu_1, \nu_2)=(540, 820)$ for $c_1(T_N)$, and $(\nu_1', \nu_2')=(970, 1130)$ for $c_2(T_N)$. The resulting fractions are displayed for both carbon dioxide and ozone in table 4.

Within the two selected band intervals specified in table 4, the product transmissivities $\bar{\tau}_F(u^*)\ \tau_F(\mathcal{U}^*)$ and $\bar{\bar{\tau}}_F(u^*)\ \tau_F(U^*)$, respectively apply. Within the *remainder* of the black body spectrum at $T=T_N$, water vapor transmissivity *alone* applies. The transmission of interface flux of the latter part of the spectrum is

$$F_{INT}(u^*) = \sigma T_N^4 \{ \tau_F(u_N^*) - c_1(T)\bar{\tau}_F(u_N^*) - c_2(T)\bar{\bar{\tau}}_F(u_N^*) \}. \quad (28)$$

In (28), $\tau_F(u_N^*)$ is the "all wave" transmissivity of water vapor (see [2], table 7). Subtraction of the second and third terms on the right side of (28) has the effect of excluding the energy transmission by water vapor alone, from the two selected band intervals.

To the interface transmission by water vapor acting without overlap must be added the transmission in the carbon dioxide and ozone band intervals. The additional interface transmission in these two intervals is

$$\sigma T_N^4 \{ c_1(T_N)\bar{\tau}_F(u_N^*)\tau_F(\mathcal{U}_N^*) + c_2(T_N)\bar{\bar{\tau}}_F(u_N^*)\tau_F(U_N^*) \}. \quad (29)$$

Addition of the two transmitted interface contributions (28, 29) leads to the total transmitted interface flux

$$F_{INT}\ (\text{trans}) = \sigma T_N^4 \{ \tau_F(u_N^*) - c_1(T_N)\bar{\tau}_F(u_N^*)\epsilon_F(\mathcal{U}_N^*) - c_2(T_N)\bar{\bar{\tau}}_F(u_N^*)\epsilon_F(U_N^*) \}. \quad (30)$$

Equation (30) may be expressed more simply in the form

$$F_{INT}\ (\text{trans}) = (\sigma T_N^4)\tau_F\ (\text{net}) \quad (31)$$

where τ_F(net) is the "net transmissivity" of the atmosphere above the interface and stands for the expression within the braces of (30). From $\epsilon_F = 1 - \tau_F$, the values of $\epsilon_F(\mathcal{U}_N^*)$ and $\epsilon_F(U_N^*)$ are readily obtained from EC tables 3 and 5 while $\tau_F(u_N^*)$ follows from EC table 7. The other parameters required for τ_F(net) are $\bar{\tau}(u_N^*)$, $\bar{\bar{\tau}}_F(u_N^*)$, $c_1(T_N)$, and $c_2(T_N)$, functional or tabular values of which have been developed in the two preceding subsections.

Values of τ_F(net), given by the expression within the braces of (30), and of $(\sigma T_N^4)\tau_F$(net) have been compiled for each sounding in columns 8 and 9, respectively, of table 2. The total emergent flux F, considering both air and interface, is listed in the final column of table 2 as the sum of the right sides of (25) and (31), and represents the desired computation by our adaptation of the EC model.

For each sounding investigated here, we have also listed a comparative value F_{WYL} in table 5, column 2. These are deduced from the emergent intensities $I(\theta)$ of the WYL 1966 computational model, furnished by Wark et al.[6] At the same time, Wark et al. provided for each model atmosphere, the NIMBUS II filtered radiances $I_2(\theta)$ and $I_4(\theta)$ in channels 2 and 4 (10–11 and 5–30 microns, respectively), as computed after appropriate use of the *effective spectral response* functions ([10], chap. 4). Our interest in these filtered intensities (radiances) lies in deriving "gross" air-mass radiative properties, which may serve as statistical predictors in the specification of either or both flux calculations considered in this study, especially, that due to the EC model.

4. COMPUTATIONS OF F_{WYL} AND OF FILTERED FLUXES IN CHANNELS 2 AND 4

The 1966 computations of intensities $I(\theta)$ due to Wark et al., available for each sounding, and at each of five zenith angles $\theta=0°, 20°, 45°, 60°, 78.5°$ are employed in connection with equation (1) to obtain values of F_{WYL}. The intensities, both unfiltered and filtered, were subject to variation with zenith angle θ, as is indicated notationally by the symbolism $I(\theta)$, $I_2(\theta)$, and $I_4(\theta)$, according to the context.

In order to derive outgoing fluxes from unfiltered radiances, we have employed the trapezoidal rule in a finite interval summation of (1). This leads to a sum consisting

[6] Private communication.

TABLE 5.—*Listing of gross parameters used in specification of the flux residual for each sounding case considered in this study. Each case number refers to the same sounding as the corresponding case of table 2.*

Case No.	F_{WYL}	ΔF	σT_N^4	ϕF_4	u_N	Pressure at interface	$\phi F_2/\pi$	$P_{en}^{.06}$
002	272.299	077.935	417.786	181.076	2.890	1000	8.827	0.81115
003	280.695	079.184	395.435	186.376	2.596	1009	8.751	0.83146
004	258.620	058.430	368.771	171.133	1.284	1014	7.797	0.87148
007	232.127	028.133	288.090	153.014	0.634	0998	6.055	0.88578
008	217.907	009.704	267.109	143.171	0.410	1000	5.440	0.87896
010	286.939	077.992	447.042	189.664	3.904	1000	9.058	0.84896
012	258.294	050.418	358.492	170.847	1.124	0923	7.524	0.80668
013	247.165	044.732	338.581	163.286	0.970	1003	6.991	0.86462
020	282.575	062.909	406.495	188.125	1.278	0850	8.734	0.75552
023	236.450	020.244	319.511	155.662	0.566	1000	6.521	0.84004
027	213.143	008.024	251.167	140.013	0.441	0941	5.021	0.79424
031	165.852	-022.446	172.884	105.440	0.117	1020	3.061	0.85945
050	248.753	007.903	324.201	164.415	0.437	0850	6.940	0.72148
051	237.274	-029.344	292.430	156.219	0.170	0850	6.216	0.69581
052	220.708	-035.317	263.054	144.776	0.161	0500	5.336	0.63201
053	247.594	-000.013	324.009	163.762	0.344	0830	6.802	0.75852
054	212.915	049.783	275.359	140.085	0.292	0703	5.430	0.63268
055	278.055	060.850	373.925	184.727	1.340	0908	8.155	0.80328
056	184.874	-046.982	217.912	120.077	0.056	0526	4.056	0.51478
057	157.051	-018.906	147.883	099.153	0.148	1006	2.578	0.78622
058	202.809	-036.677	247.293	133.449	0.158	0400	4.902	0.39439
059	274.038	076.239	406.495	181.957	2.637	0850	8.433	0.73187
060	216.018	-029.592	263.054	141.883	0.202	0500	5.295	0.47760
061	264.099	045.098	363.604	175.614	1.112	0700	7.612	0.62699
062	245.319	001.816	319.511	162.747	0.418	0652	6.623	0.61077
063	269.466	014.935	363.604	178.669	0.506	0754	7.735	0.68489
064	153.857	-042.597	158.633	096.914	0.012	0400	2.743	0.39179
065	217.730	012.329	288.090	143.358	0.630	0100	5.720	0.61461
066	220.581	006.729	283.798	145.276	0.526	0700	5.661	0.61810
067	213.778	-027.934	263.054	140.226	0.195	0568	5.196	0.54156
068	166.521	-047.362	181.883	106.511	0.036	0500	3.248	0.45402
069	184.217	-039.695	214.432	119.152	0.096	0700	3.990	0.61249
070	188.841	-039.359	221.434	122.381	0.102	0700	4.141	0.60943
071	221.462	-019.144	275.359	146.354	0.287	0476	5.663	0.46042
072	230.074	-032.356	279.555	151.586	0.186	0466	5.815	0.45652
073	249.914	062.574	348.430	165.731	1.232	0700	7.364	0.60671
074	266.591	065.191	373.993	176.863	1.824	0810	8.002	0.53130
075	282.114	064.035	395.435	187.088	1.367	0930	8.561	0.83890
076	248.626	053.370	328.942	164.492	1.525	0932	7.073	0.77845
077	212.865	-036.982	243.469	138.983	0.135	0500	5.028	0.47086
078	202.028	-040.510	232.255	131.614	0.107	0500	4.644	0.48074
079	184.081	-044.935	200.929	110.779	0.068	0400	3.899	0.37214
080	236.346	008.362	292.430	155.021	0.497	0806	6.267	0.68859
081	177.815	-048.485	194.420	114.152	0.040	0500	3.612	0.47247
082	159.412	-044.142	167.073	101.118	0.027	0400	2.985	0.37013
083	219.682	-001.647	275.259	144.337	0.361	0800	5.529	0.70843
084	218.273	-023.263	271.210	143.031	0.258	0722	5.438	0.66017
085	220.480	000.544	283.798	145.922	0.443	0700	5.814	0.62960
086	180.130	-037.778	214.432	116.863	0.098	0720	4.025	0.62791
087	128.578	-034.003	135.224	079.778	0.007	0400	2.080	0.34384
088	182.125	-041.775	214.432	117.937	0.069	0818	3.969	0.72435
089	188.324	-047.601	207.598	131.593	0.053	0500	4.016	0.47676
090	200.924	-053.220	224.998	130.516	0.038	0370	4.413	0.36765
091	294.465	086.599	459.165	193.003	2.843	1000	9.775	0.84952
092	268.189	048.202	368.771	178.260	1.174	0700	7.862	0.62831
093	264.221	044.096	363.604	175.544	1.076	0700	7.803	0.62469
094	275.908	068.839	395.435	183.440	1.765	0850	8.360	0.51059
095	251.459	038.199	338.581	167.003	1.021	0700	7.018	0.62786
096	270.866	-034.780	373.993	180.008	0.894	0850	7.929	0.36623
097	262.837	054.533	358.492	174.560	1.264	0850	7.609	0.76870
098	247.791	004.764	314.872	163.219	0.428	0724	6.717	0.66450
099	239.441	010.425	305.746	158.044	0.547	0900	6.297	0.76243
100	203.470	-023.645	239.687	132.669	0.203	0700	4.699	0.58719

of five terms, the last of which has the form

$$\delta F=\pi\left[\frac{I(78.5°)+I(90°)}{2}\right](\sin^2 90°-\sin^2 78.5°) \quad (32)$$

with $I(90°)$ to be determined by the procedure of the next paragraph. The flux contribution by (32) ranged between 2–3 percent of the total of the five terms

$$F_{WYL}=\pi\left\{\left[\frac{I(0)+I(20°)}{2}\right](\sin^2 20°-0)+\ .\ .\ .\right.$$
$$\left.+\left[\frac{I(60°)+I(78.5°)}{2}\right](\sin^2 78.5°-\sin^2 60°)\right\}+\delta F. \quad (33)$$

The use of the trapezoidal rule in this way was made subject to an assumption regarding the evaluation of $I(90°)$, namely that $I(\theta)$ was computable by a Lagrangian interpolating quadratic in θ. This formulation for $I(\theta)$ as a quadratic polynomial in θ incorporated the requirement that $I(\theta)$ assume the values $I(45°)$, $I(60°)$, $I(78.5°)$ at $\theta=$ 45°, 60°, 78.5° in order to extract the maximum information regarding limb darkening into the intensity function $I(\theta)$. The resulting quadratic expression for $I(\theta)$ accurately simulated the limb-darkening effects over the range $45°\leq\theta\leq 78.5°$ for the model atmospheres shown in curves 1 to 6 in figure 4 of [13]. The quadratic expression for $I(\theta)$, when extrapolated to $\theta=90°$ gave the result

$$I(90°)=2.1783\,I(78.5°)-1.8649\,I(60°)+.6846\,I(45°) \quad (34)$$

which was used in (32), (33). The polynomial $I(\theta)$, valid in the range $45°\leq\theta\leq 78.5°$, was reasonably realistic in the range $\theta>78.5°$, as evidenced by a more rapid rate in the limb-darkening effect, which increased proportionately to θ^2 for $\theta>78.5°$. The contribution of δF computed by (32) and (34) was, furthermore, acceptably below the 4 percent upper limit to the total flux attributable to the conical volume lying beneath the zenith angle 78.5° (WYL [13]). The use of the trapezoidal rule in a finite difference sense appeared to give rise, at worst, to very small truncation error because of the smooth decrease of $I(\theta)$ with increasing θ. For these reasons, F_{WYL} was taken to be uniquely and accurately determined by equation (33) supplemented by (34). It was thus possible to compute the flux residual ΔF resulting from the two methods of computation, defined by

$$\Delta F=F_{WYL}-F \quad (35)$$

where F is the result of our computational model (section 3), and F_{WYL} results from equation (33).

Based upon correlation studies similar to those to be described in section 5, simple correlation coefficients in excess of 0.99 have been found to exist between the 1966 unfiltered and filtered radiances of WYL. This statement applies to $I(\theta)$ taken pairwise with either $I_4(\theta)$ or $I_2(\theta)$. As a result, equations (32), (33), (34) were used to compute "filtered fluxes" ϕF_4 and ϕF_2, for channels 4 and 2, simply by replacing $I(\theta)$ by $I_4(\theta)$ and $I_2(\theta)$, respectively. These filtered fluxes are listed in table 5, in columns 5 and 8 respectively. For computational convenience ϕF_2 has been left scaled by the factor $(1/\pi)$ in column 8.

5. STATISTICAL SPECIFICATION OF THE COMPUTED FLUXES AND OF THE FLUX RESIDUAL

In section 3, we generated fluxes F (column 10, table 2) based upon the EC model. Values of F_{WYL}, and of ΔF by (35), have also been derived in section 4. Comparative flux values F and F_{WYL} are studied in this section. There is no *a priori* knowledge of which model gives the most representative results. In consequence, we have made use of linear regression techniques, employing gross scale radiative parameters representative of the model atmospheres, in order to determine the degree of specification of F_{WYL} and F in terms of empirically based independent variables. The independent variables defined for this purpose are

$$X_1=\sigma T_N^4;\ X_2=\phi F_4;\ X_3=\phi F_2;$$
$$X_4=u_N P_{eN}^{.85};\ X_5=(.01p_N)P_{eN}^{.85}.$$

The variables X_1, X_4, X_5 are representative of the gross radiative properties of the sounding itself. Kuhn [6], and Kuhn and Suomi [7] have suggested from radiometersonde data the forms of X_4 and X_5, apart from the arbitrary constant of proportionality in X_5. The use of X_1 is suggested by the fact that it is singly the most representative measure of flux contained within the sounding. The other two variables, X_2 and X_3, normally are satellite-sensed gross radiative parameters. In the computational test conducted in this study, however, X_2 and X_3 were computed, and bear close to a linear relationship to F_{WYL} through the effective response functions used for their selected regions of the spectrum ([10], chap. 4). This quasi-linear relationship is further borne out in table 6, which lists correlation coefficients between F_{WYL} and X_2 of 0.980, and of 0.975 in the case of F_{WYL} and X_3.

TABLE 6.—*Matrix of the simple correlation coefficients* ($Y=F_{WYL}$, $y=F$ by EC method, $\mathcal{Y}=\Delta F$)

	X_1	X_2	X_3	X_4	X_5	Y	y	$\mathcal{Y}$
X_1	1.000	.981	.997	.795	.522	.970	−.005	.861
X_2	.981	1.000	.989	.705	.499	.980	.092	.817
X_3	.997	.989	1.000	.770	.520	.975	.011	.858
X_4	.795	.705	.770	1.000	.599	.697	−.337	.802
X_5	.522	.499	.599	.520	1.000	.494	−.408	.661
Y	.970	.980	.975	.697	.494	1.000	.087	.838
y	−.005	.092	.011	−.337	−.408	.087	1.000	−.471
$\mathcal{Y}$	.861	.817	.858	.802	.661	.838	−.471	1.000

The variable P_{eN} appearing in both X_4 and X_5 is the effective pressure of both of the optical masses u_N and cp_N, of water vapor and carbon dioxide, respectively, of the full depth of the atmospheric model, and is derived from equation (2). The constant c is $(.4764/g\rho_0)$, but may be replaced by the arbitrary constant 0.01, for its use in the regression analysis conducted here. In table 5, the sample values u_N, p_N, $P_{eN}^{.85}$ have been listed, the parameters X_4 and X_5 having been transgenerated by an option of the computer stepwise regression program.

The Miller [9] stepwise regression technique analyzes the explained variance in Y (or y, $\mathcal{Y}$) by each independent variable X_i added to the regression equation:

$$Y=A_0+\sum_{k=1}^{i} A_i X_i, \qquad i=1, \ldots, 5. \quad (36)$$

The final selection of the X_i's are arranged in order of descending values of "$\mathcal{F}^k$ upon entry" after the kth entry has been made, where the definition of $\mathcal{F}^k$ is given by

$$\mathcal{F}^k=\frac{[\text{total M.S. expl., step } k]-[\text{total M.S. expl., step } k-1]}{[\text{mean square unexplained by (36) at step } k]}. \quad (37)$$

In addition, to insure that the final regression be significant at the 95 percent confidence level, Miller requires that each $\mathcal{F}^k$ exceed the *critical* $\mathcal{F}_c^k$ defined for the kth step as

$$\mathcal{F}_c^k=\mathcal{F}_{\alpha/k}[1, N-k-1]. \quad (38)$$

From the simple correlation $R(X_1, X_3)=0.997$ of table 6, it is evident that only negligible added explained variance can be derived from the inclusion of both X_1 and X_3 in the same stepwise regression. Hence the maximum k considered is 4. For this choice of k, and with the sample size $N=63$, $\mathcal{F}_c^k$ is conservatively set at

$$\mathcal{F}_c^{(4)}=\mathcal{F}_{.05/4}[1, 58]=6.64. \quad (39)$$

TABLE 7.—*Results of the stepwise, screening regression process applied to the specification of* (a) $Y=F_{WYL}$; (b) $y=F$; (c) $\mathcal{Y}=\Delta F$; (d) X_2; (e) X_3

Dep. vrbl.	Step number	Predictor X_k added	Std. dev. of X_k	% cum. red. variance	$\mathcal{F}^k$ upon entry of X_k	Coeff of X_k	Statistics at final significant entry in equation (36): Mult. correl. coeff.	Std. error est.
(a) Y	1	X_2	72.8057	.9606	1487.49	1.41187	.9801	7.8741 wm^{-2}
	2*	X_1	27.3173	.9623	2.6929			
	3	X_4	.62359	.9635	1.8869			
	4	X_5	2.33542	.9636	.1069			
		Constant term				17.34933		
(b) y	1	X_5	2.33542	.1664	12.1792	−5.33358	.6650	18.6472
	2	X_2	27.3173	.2827	9.7298	2.15490		
	3	X_1	72.8057	.4423	16.8756	−.65895		
	4*	X_4	.67359	.6616	2.0842			
		Constant term				119.17853		
(c) $\mathcal{Y}$	1	X_1	72.8057	.7420	175.430	.50840	.8962	20.0443
	2	X_5	2.33542	.8032	18.6415	2.07926		
	3*	X_2	27.3173	.8184	4.9458			
	4	X_4	.67359	.8209	.8097			
		Constant term				−64.64534		
(d) X_2	1	X_3	5.84533	.9786	2785.245	5.10958	.9933	3.2381
	2	X_4	.67359	.9864	34.545	−0.00410		
	3*	X_5	2.33542	.9866	1.0162			
		Constant term				55.19379		
(e) X_3	1	X_1	72.8057	.9937	9579.264	.61847	.9975	0.4181
	2	X_4	.67359	.9950	15.573	−5.625		
	3*	X_5	2.33542	.9951	1.880			
		Constant term				−3.99456		

In applying the computer version of the stepwise regression program the variables X_2, X_4, X_5 and only one of X_1 or X_3 were used in the specification of $Y=F_{WYL}$, $y=F$ by the EC method, and of ΔF of (35). In parts (d) and (e) of table 7, the results of the screening regression of the variables X_2 and X_3 in terms of the radiosonde-derived parameters X_1, X_4, and X_5 are shown. In table 7, all five sets of specifications have been summarized, and the first step number at which a listed X_k fails to exceed $\mathcal{F}_c^{(4)}$ of (39) is marked by an asterisk superscript; and the coefficient column is left blank at this and succeeding steps. The final column of table 7 lists the multiple correlation coefficient and the standard error of estimate after application of the final screened version of the multiple regression equation. In each of the cases (a), . . ., (e), the appropriate equation is generated from the column of coefficients of X_k of table 7, including the *constant term* applicable at the step of entry of the last significant variable introduced.

It is clear from table 7, that the use of the independent variables X_1, . . ., X_5 gives much higher specification of F_{WYL} than of $y=F$ by the EC model. The comparative results for the WYL and EC cases, respectively are

$$Y=1.73493+1.41187X_2, \qquad R_{Y.X_2}=0.9801$$

$$y=119.17853-5.33358X_5+2.15490X_2-0.65895X_1,$$

$$R_{Y.521}=0.6650. \quad (40)$$

In view of the results of sections (d) and (e) of table 7, it is clear that both Y and y may be specified with nearly as much significance by deleting the filtered fluxes X_2 and X_3 from the analysis. If this is done the comparative results may be written in the semistandardized form

$$Y-228.6502=0.56790(X_1-293.6907)$$

$$-12.7157(X_4-0.52631), \qquad R_{Y.14}=0.9770$$

$$y-220.8306=0.23805(X_1-293.6907)$$

$$-25.8997(X_4-.52631)-3.9258(X_5-5.01092),$$

$$R_{Y.145}=0.6254 \quad (41)$$

in terms of the *empirically based* air mass properties X_1, X_4, X_5 alone. In both (40), (41) all variables X_k selected are at a confidence level prescribed by $\mathcal{F}_c^k$ of (39), or higher.

The regression which reveals most expressively the bias between the sets of results (Y, y) is that for $\mathcal{Z}=F_{WYL}-F$, summarized in table 7(c). In semistandardized form, this *screened* regression assumes the form

$$\mathcal{Y}-7.81959=0.50840(X_1-293.6907)$$

$$+2.07926(X_5-5.01092), \qquad R_{Y.15}=0.8962. \quad (42)$$

Equation (42) shows that for values of X_1 and X_5 both well below their sample means, $\mathcal{Y}$ can be negative, that is for cold interfaces and shallow atmospheric depths, F by the EC model will exceed F_{WYL}. The reverse is true for

$$X_1>293.6907 \text{ and } X_5>5.01092.$$

Equation (42) has a multiple correlation coefficient of

0.8962 but has also a sizeable standard error of estimate, so that these conclusions are somewhat tentative. Nevertheless, this bias in the Elsasser-Culbertson emissivities is consistent with those reported by several investigators whose emissivity functions have been summarized by Kuhn [6] in his figure 5.

6. CONCLUSIONS

A new computational model for estimating emergent terrestrial flux, based upon the Elsasser-Culbertson monograph [2] is presented here. Computations have been made for a set of 63 model atmospheres listed in Wark et al. [13], and comparisons made with results of the latter authors for the same set of atmospheres. For verifications of both sets of computational models, the fluxes have been specified statistically in terms of empirically based variables descriptive of certain large-scale features of the soundings. The final variables employed are X_1, X_4, and X_5, listed in the first paragraph of section 5. After use of the Miller [9] stepwise screening technique to eliminate insignificant predictors, it was found that 95.45 percent of the variance of F_{WYL} was explained, while only 38.22 percent of the flux by the EC model was explained by these same variables. The screening technique also revealed a bias in $F_{WYL}-F$ such that the difference tends to be positive for a warm, deep atmosphere, with a reverse tendency for cold, shallow atmospheres. The existence of such a bias has been found by other investigators, but its degree of specification *in this study* was somewhat limited by the limited vertical resolution in the soundings used. It is recommended that in future operational use of the EC model, the atmosphere be divided into layers of 50 mb. or smaller below 400 mb., and of 25 mb. or smaller above 400 mb.

For the case of uniform interface temperatures considered here, the filtered fluxes ϕF_2, ϕF_4 in channels 2 and 4, were very nearly related statistically, by a linear relationship with F_{WYL}. It would be an interesting experiment to determine the relative specifications of the two computational systems applied to scattered-to-broken middle clouds, using mean cloud element depth to width ratio as an additional air-mass parameter.

ACKNOWLEDGMENTS

Appreciation is due to Miss Sharon Raney who assisted in numerous aspects of the programming. Also our thanks are expressed to Mrs. Ruth Guthrie for her careful typing of the manuscript.

REFERENCES

1. T.G. Cowling, "Atmospheric Absorption of Heat Radiation by Water Vapour," *Philosophical Magazine*, London, vol. 41, No. 313, Feb. 1950, pp. 109–123.
2. W. M. Elsasser and M. F. Culbertson, "Atmospheric Radiation Tables," *Meteorological Monographs*, American Meteorological Society, Boston, vol. 4, No. 23, Aug. 1960, pp. 1–43.
3. R. M. Goody, "A Statistical Model for Water-Vapour Absorption," *Quarterly Journal of the Royal Meteorological Society*, vol. 78, No. 336, Apr. 1952, pp. 165–169.
4. R. M. Goody, *Atmospheric Radiation I*, Oxford Press, London, 1964, 436 pp.
5. R. A. Hanel, W. R. Bandeen, and B. J. Conrath, "The Infrared Horizon of the Planet Earth," *Journal of the Atmospheric Sciences*, vol. 20, No. 2, Mar. 1963, pp. 73–86.
6. P. M. Kuhn, "Radiometersonde Observations of Infrared Flux Emissivity of Water Vapor," *Journal of Applied Meteorology*, vol. 2, No. 3, June 1963, pp. 368–378.
7. P. M. Kuhn and V. E. Suomi, "Airborne Radiometer Measurements of Effects of Particulates on Terrestrial Flux," *Journal of Applied Meteorology*, vol. 4, No. 2, Apr. 1965, pp. 246–252.
8. F. L. Martin and W. C. Palmer, "Statistical Estimates of Computed Water-Vapor Radiative Flux from Clear Skies at an Oceanic Location," *Journal of Applied Meteorology*, vol. 3, No. 6, Dec. 1964, pp. 780–787.
9. R. G. Miller, "Statistical Prediction by Discriminant Analysis," *Meteorological Monographs*, American Meteorological Society, Boston, vol. 4, No. 25, Oct. 1962, pp. 1–54.
10. Staff members, *NIMBUS II User's Guide*, Laboratory for Atmospheric and Biological Sciences, Goddard Space Flight Center, National Aeronautics and Space Administration, NASA, Greenbelt, Md., 1966, 229 pp.
11. S. L. Valley (Scientific Editor), *Handbook of Geophysics and Space Environments*, Air Force Cambridge Research Laboratories, L. G. Hanscom Field, Bedford, Mass., 1965.
12. C. D. Walshaw, "Integrated Absorption by the 9.6 μ Band of Ozone," *Quarterly Journal of the Royal Meteorological Society*, vol. 83, No. 357, July 1957, pp. 315–321.
13. D. Q. Wark, G. Yamamoto, and J. H. Lienesch, "Infrared Flux and Surface Temperature Determinations From TIROS Radiometer Measurements," *Report* No 10, Meteorological Satellite Laboratory, U.S. Weather Bureau, Washington, D.C., Aug. 1962, 84 pp. (model atmospheres included in the Appendix), Supplement added, Apr. 1963, 7 pp.
14. D. Q. Wark, G. Yamamoto, and J. H. Lienesch, "Methods of Estimating Infrared Flux and Surface Temperatures From Meteorological Satellites," *Journal of the Atmospheric Sciences*, vol. 19, No. 4, Sept. 1962, pp. 369–384.

[Received October 10, 1967; revised March 25, 1968]